

# Clifford Kolmogorov-Arnold Networks

Matthias Wolff

Department of Computer Science  
*University of Münster*  
 Münster, Germany  
 0009-0006-1432-6265

Francesco Alesiani

*NEC Laboratories Europe GmbH*  
 Heidelberg, Germany  
 0000-0003-4413-7247

Christof Duhme

Department of Computer Science  
*University of Münster*  
 Münster, Germany  
 0009-0004-1853-2862

Xiaoyi Jiang

Department of Computer Science  
*University of Münster*  
 Münster, Germany  
 0000-0001-7678-9528

**Abstract**—We introduce Clifford Kolmogorov-Arnold Network (CIKAN), a flexible and efficient architecture for function approximation in arbitrary Clifford algebra spaces. We propose the use of Randomized Quasi Monte Carlo grid generation as a solution to the exponential scaling associated with higher dimensional algebras. Our CIKAN also introduces new batch normalization strategies to deal with variable domain input. CIKAN finds application in scientific discovery and engineering, and is validated in synthetic and physics inspired tasks.

**Index Terms**—Kolmogorov-Arnold Networks, Complex-Valued Neural Networks, Hypercomplex Neural Networks

## I. INTRODUCTION

The Kolmogorov-Arnold Representation Theorem (KAT) [1] provides an alternative way of representing functions of multiple variables, including continuous and discontinuous functions [2]. While it is a useful theoretical tool, its application was only marginally explored [3]. After Liu et al. [4] have recently sparked new interest in the field proposing Kolmogorov-Arnold Networks (KANs), there has been a surge of extensions as well as applications of this new architecture [5]. Especially for function fitting tasks, KANs have shown to be a promising alternative to conventional Multilayer Perceptrons (MLPs) [6] while also offering intrinsic interpretability.

Wolff et al. [7] have transferred the advantages of KANs into the field of Complex-Valued Neural Networks (CVNNs) and introduced a Complex-Valued Kolmogorov-Arnold Network (CVKAN) by making use of Radial Basis Functions (RBFs). Che et al. [8] have then adapted the underlying KAT to the complex domain with mathematical proofs and further improved the CVKAN by changing the residual activation function and making the shape of the RBFs learnable.

However, scientific discovery, engineering, computer vision or robotic applications work with high dimensional representations, for example, to describe electromagnetic fields, weather state variables, 3-dimensional objects, or multi-joint robot arms. In these scenarios, complex numbers are not sufficient.

This work has been submitted to the IEEE for possible publication. Copyright may be transferred without notice, after which this version may no longer be accessible.

In this work we therefore propose Clifford Kolmogorov-Arnold Network (CIKAN), an extension to CVKAN for higher dimensions than complex numbers. By increasing the dimensionality of the grid on which the RBFs are defined and using the geometric product defined in the Clifford Algebra (CA), we can learn a function on each edge connecting two nodes in the CIKAN that maps from  $\mathbb{C}l \mapsto \mathbb{C}l$ , similar to KAN and CVKAN that map from  $\mathbb{R} \mapsto \mathbb{R}$  or  $\mathbb{C} \mapsto \mathbb{C}$ , respectively.

Overall our contributions can be summarized as:

- We extend the CVKAN framework [7] to the hyper-complex domain using Clifford algebras (Section IV).
- We propose two different type of RBFs as function basis (Section IV-A).
- We propose to transition from a uniform grid to a randomly sampled grid to mitigate the curse of dimensionality. In particular, we introduce the use of Randomized Quasi Monte Carlo (RQMC) *scrambled Sobol sequence* for the grid generation (Section IV-C).
- We show the expressivity of the proposed approach when using the *Sobol grid* (Section IV-D).
- We study the effect of different batch normalization techniques suitable for Clifford domain and KAN architecture in general (Section IV-E).
- We will provide our code of the model and the experiments as an open source library to promote open science.<sup>1</sup>

In addition, we evaluate (Section V) CIKAN against the conventional CVKAN (described in Section III-B) in complex-valued experiments, we study the influence of different batch normalization strategies, and the use of the proposed RBFs (Section V-A and Section V-B). Further, we study the suitability of our proposed CIKAN with higher dimensional CAs (introduced in Section III-A), e.g. quaternions,  $\mathbb{C}l(2)$ ,  $\mathbb{C}l(1,1)$ , in synthetic function fitting tasks. We show that our proposed *Sobol grid* approach is helpful for reducing the number of parameters (Section V-C), while providing flexible performances.

<sup>1</sup>Link to code base: <https://github.com/M-Wolff/CliffordKAN>

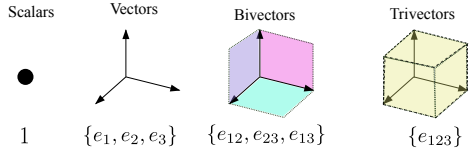


Fig. 1: Visualization of  $\mathbb{C}l(3)$  grades (scalars, vectors, bivectors and trivectors).

## II. RELATED WORK

### A. Kolmogorov-Arnold Function Representation

Kolmogorov-Arnold function representation theorem provides an alternative tool for function approximation [9], with the potential to address the curse of dimensionality [10]. The original KAN architecture has been extended to Convolutional Neural Networks (CNNs) [11], [12], and to transformer models [13]. To apply KANs to PolSAR classification, [14] developed a complex-valued convolutional KAN. Furthermore, matrix group equivariance has been integrated into the KAN architectural [15], while [16] provides an extension for geometrical symmetries and invariance. Adaptive KAN architecture [17] reduces the need for hyperparameter optimization. Liu et al. [18] explore the use of KANs in science with symbolic regression. While [7], [8] explore the applied and theoretical aspects of complex KAN, and [19] studies the role of residual connections.

### B. Clifford Algebra

Clifford's Geometric Algebra (GA) provides a powerful mathematical tool for describing spatial relationships and transformations. GA generalizes complex numbers and quaternions into a unified system [20]. CA has found application in modeling Partial Differential Equations (PDEs) [21] or in modeling rotational and translation ( $E(3)$ ) or Lorentz ( $O(1, 3)$ ) symmetries [22]–[24], which are used to describe interactions in physical systems. Conformal Geometric Algebra (CGA) is used in robotic vision [25], for inverse kinematics [26], or in computer vision [27].

## III. BACKGROUND

### A. Clifford algebra

Clifford algebra [20], [23], [28] extends Euclidean vector space to a full algebra by introducing the concept of geometric product. Clifford algebra finds application in various areas of mathematics, physics, science, and engineering. If  $V$  is a finite-dimensional vector space of dimension  $n = \dim V$ , over a field  $\mathbb{F}$  ( $\mathbb{R}$  in the paper) equipped with a quadratic form  $q : V \rightarrow \mathbb{F}$ , then  $\mathbb{C}l(V, q)$  is the Clifford Algebra, a unitary, associative, noncommutative algebra generated by  $V$ , where  $v^2 = q(v)$ . Each element of the algebra is a linear combination of a finite product of vectors  $v_{ij} \in V$ ,

$$x = \sum_{i \in I} c_i v_{i,1} \dots v_{i,k_i},$$

with  $c_i \in \mathbb{F}$ ,  $k_i \in N_0$ ,  $I$  finite.

The bilinear form associated with  $\mathbb{C}l(V, q)$  is defined as  $b(v_1, v_2) = \frac{1}{2}(q(v_1 + v_2) - q(v_1) - q(v_2))$ , which satisfy the identify  $v_1 v_2 + v_2 v_1 = 2b(v_1, v_2), \forall v_1, v_2 \in V$ . This defines the *geometric product*  $v_1 v_2$  on which the algebra is defined. If  $v_1, v_2$  are orthogonal then  $b(v_1, v_2) = 0$  and therefore  $v_2 v_1 = -v_1 v_2$ . If  $e_1, \dots, e_n$  is an orthogonal basis of  $V$ , then the set of tuples  $e_I = e_{i_1} \dots e_{i_{|I|}}, I = (i_1, \dots, i_{|I|}) \subseteq [n]$  forms an orthogonal basis for  $\mathbb{C}l(V, q)$ . Therefore, the dimension of the Clifford Algebra is  $D = \dim \mathbb{C}l(V, q) = 2^n$ . We can partition the algebra into vector spaces  $\mathbb{C}l^{(m)}(V, q), m = 0, \dots, n$  called *grades* (see Fig. 1), where the  $\dim \mathbb{C}l^{(m)}(V, q) = \binom{n}{m}$ . Notably,  $\mathbb{C}l^{(0)}(V, q) = \mathbb{F}$ , and  $\mathbb{C}l^{(1)}(V, q) = V$ . The elements of  $\mathbb{C}l^{(2)}(V, q)$  and  $\mathbb{C}l^{(3)}(V, q)$  are called bivectors and trivectors, while  $\mathbb{C}l^{(n)}(V, q)$  contains the pseudoscalar. The bilinear operator implies the scalar product  $x \cdot y = b(x, y) = \frac{1}{2}(xy + yx), x, y \in \mathbb{C}l(V, q)$ , similarly we can define the external product as  $x \wedge y = \frac{1}{2}(xy - yx)$ . We can now write the geometric product between two vectors  $v, u \in V$  as

$$vu = v \cdot u + v \wedge u$$

The resulting object has two components, a scalar  $v \cdot u$  and a bivector  $v \wedge u$ , which represents an area. When CA is used in e.g. describing the Maxwell's equations [29], the electric and magnetic fields can be represented as a single element in the algebra, with  $F = E + e_{123}cB$ , with  $E$  and  $B$  the electric and magnetic vectors, while  $e_{123}$  is the pseudo-scalar and  $c$  is the light speed. Further notice that the element  $e_{123}cB$  is a bivector. We can now write, from the original 12 equations, the Maxwell's equations as  $(1/c\nabla_t + \nabla_x)F = 1/\epsilon_0(\rho - J/c)$ , where  $\rho, J$  represent charges (scalar) and the electric currents (vector), and  $\epsilon_0$  the dielectric constant. For convenience, we refer to the Clifford Algebra as  $\mathbb{C}l(p, q, r)$ ,  $\mathbb{C}l_{p,q,r}$ , or simply  $\mathbb{C}l$ , where the triplet  $(p, q, r)$  counts the number of elements that square to 1, -1 and 0, i.e.  $q(e_i) = \{1, -1, 0\}$ .

Notable examples of Clifford Algebras are the Euclidean Geometric Algebra (EGA), for example  $\mathbb{C}l(2)$  is used in PDE to model weather [21], or  $\mathbb{C}l(3)$  is used to model Maxwell's equations [29]. The Projective Geometric Algebra (PGA)  $\mathbb{C}l(3, 0, 1)$  and the Conformal Geometric Algebra (CGA)  $\mathbb{C}l(4, 1)$  are used for computer vision [25], and robotic manipulation [26] applications. The Spacetime Algebra  $\mathbb{C}l(3, 1)$  describes the Minkowski space and is used to model relativistic physics [30].

### B. Complex-valued Kolmogorov-Arnold Network

Wolff et al. [7] extended the KAN [4] framework to the complex domain with the CVKAN inspired by the CVNN, which are known for improved generalization in signal processing and physics-related tasks. CVKAN introduces the complex RBF as the base function of the expansion of the univariate function for the KAN architecture. The Complex RBF  $\phi_{\mathbb{C}} : \mathbb{C} \rightarrow \mathbb{R}$  is defined as  $\phi_{\mathbb{C}}(x) = \exp(-|x|^2)$ , with  $|x|$  the absolute value of the complex number  $x \in \mathbb{C}$ , and centered on a regular grid in  $\mathbb{C}$ , i.e. grid points  $g \in \mathbb{C}$ , resulting in the univariate function of the form

$\Phi_{\mathbb{C}}(x) : \mathbb{C} \rightarrow \mathbb{R} = \sum_{g \in G} w_g \phi_{\mathbb{C}}(x - g)$ . CVKAN also introduces  $\mathbb{C}\text{Sigmoid Linear Unit}$  (SiLU), complex nonlinearity, defined as  $\mathbb{C}\text{SiLU} = w(\text{SiLU}(\Re(x)) + i\text{SiLU}(\Im(x))) + \beta$ , where  $w, \beta \in \mathbb{C}$  are a learnable weight and bias, and  $\Re(x)$  and  $\Im(x)$  are the real and imaginary part of  $x \in \mathbb{C}$ , and  $\text{SiLU}(x) = x(1 + e^{-x})^{-1}$ .

#### IV. METHODOLOGY

In this section, we describe how a  $\mathbb{C}\text{KAN}$  is constructed for any Clifford algebra  $\mathbb{C}l(p, q, r)$ . The choice of  $n = p + q + r \in \mathbb{N}_+$  defines specific algebras (Section III-A). This algebra is then used for all RBFs inside the whole  $\mathbb{C}\text{KAN}$  and dictates the rules for all other calculations, e.g. multiplication with weights.

##### A. $\mathbb{C}l\text{KAN Radial Basis Functions}$

Similar to CVKAN [7] we define a *naive RBF* (1a) with  $x \in \mathbb{C}l$  and  $\|x\|$  representing the Clifford algebra  $\mathbb{C}l$  norm of  $x$ . This formulation for our naive RBF corresponds to a mapping of  $\phi(x) : \mathbb{C}l \rightarrow \mathbb{R} = \mathbb{C}l^{(0)}$ . By using this mapping, the high-dimensional Clifford algebra space is represented by a real-valued number, the output of the RBF, therefore potentially losing information about the rich structure of the input space.

We thus propose the alternative *Clifford RBF* (1b) that retains information about the spatial properties of the Clifford-valued input. We achieve this by multiplying the output of the RBF with the input itself. The product of an element in  $\mathbb{C}l$  by a real number is still an element of  $\mathbb{C}l$ , and represents the scaled version of its components.

$$\phi(x) = \exp(-\|x\|^2) \quad (1a) \quad \phi(x)_{\mathbb{C}l} = x \phi(x) \quad (1b)$$

Equation (1b) then constitutes a mapping  $\phi(x)_{\mathbb{C}l} : \mathbb{C}l \rightarrow \mathbb{C}l$  and the output is equal to the input  $x \in \mathbb{C}l$  weighted by the real-valued output of naive RBF  $\phi(x)$ .

Following CVKAN, for  $x \in \mathbb{C}l$  is  $\mathbb{C}l\text{SiLU}$  the residual activation function with learnable weight and bias  $w, \beta \in \mathbb{C}l$ :

$$\mathbb{C}l\text{SiLU}(x) = w\text{SiLU}_{\mathbb{C}l}(x) + \beta \quad (2)$$

where  $\text{SiLU}_{\mathbb{C}l}$  denotes the dimension-wise application of the SiLU function.

##### B. $\mathbb{C}l\text{KAN uniform grid}$

To construct a learnable activation function  $\mathbb{C}l \rightarrow \mathbb{C}l$ , we need to combine multiple RBFs. The RBFs have to be centered around grid points, so we need to define a grid where each grid point  $g$  is also an element of the same underlying Clifford algebra  $g \in \mathbb{C}l$ .

In CVKAN for complex numbers this grid was defined as a uniform grid with  $N_g \times N_g$  grid points  $g \in \mathbb{C}$  within some fixed ranges, e.g.  $[-2 - 2i, 2 + 2i]$ , to likely fall inside the grid of the next layer after batch normalization changes the distribution

to  $\mu = 0, \sigma = 1$ . This also allows to use a fixed grid range and not rely on grid extension [4], [31] or learnable grid offsets [32] that might slow down or complicate the learning process.

This approach can be intuitively transferred to  $\mathbb{C}l\text{KAN}$ . Let  $D$  be the dimensionality of Clifford algebra  $\mathbb{C}l$ . For example  $D = 2$  for complex numbers and  $D = 4$  for quaternions. Then the grid  $G$  consists of  $(N_g)^D$  grid points  $g \in \mathbb{C}l$ . If we adopt the  $N_g = 8$  number of grid points per dimension from CVKAN, then for quaternions we end up with a grid of size  $8^4 = 8 \times 8 \times 8 \times 8$  and a total of 4096 grid points  $g \in \mathbb{C}l(0, 2)$ .

Consistent with CVKAN each grid point  $g \in G$  is associated with a RBF centered around it and thus a learnable weight  $w_g \in \mathbb{C}l$  that controls the influence of the RBF at grid point  $g$  on the learnable activation function. The RBF to use can either be the naive (1a) or the Clifford RBF (1b) to construct the learnable activation function (3) or (4), respectively.

$$\Phi(x) = \sum_{g \in G} w_g \phi(x - g) \quad (3)$$

$$\Phi_{\mathbb{C}l}(x) = \sum_{g \in G} w_g \phi_{\mathbb{C}l}(x - g) \quad (4)$$

If we use a uniform grid, also referred to as *full grid*, the number of learnable weights increases exponentially with the number of dimensions in the Clifford algebra (Section III-A). Therefore, we propose an alternative grid generation approach that mitigates the curse of dimensionality.

##### C. RQMC Sobol Grid

To reduce the number of trainable parameters, we introduce a random grid approach. For each dimension of  $g \in \mathbb{C}l(p, q, r)$  we sample a random number inside a fixed grid range, e.g.  $[-2, +2]$ , and repeat this process for all of the grid points. Similar to how random search was shown to be a better approach than grid search for hyperparameter optimization [33], we aim to achieve a sufficient coverage of the hypercube of all possible grid points  $[-2, +2]^D$  while requiring less grid points than the full grid approach. The sampled grid points act like supports for our learnable activation function  $\Phi(x)$  or  $\Phi_{\mathbb{C}l}(x)$ . A natural requirement for these points is to cover the hypercube evenly, for each realization, and not only in expectation. However, we noticed that naively sampled random grid points do not necessarily show this property. We therefore introduce the RQMC scrambled Sobol sequence grid, or *Sobol grid*, where we generate the grid points using quasi-random Sobol sequence [34], [35].

As shown in Fig. 2, these quasi-random numbers cover the space more evenly than true random numbers and therefore are better suited for our sampling of grid points. We call this variant of the model the Sobol Clifford Kolmogorov-Arnold Network (Sobol-CliffordKAN). In our experiments, we only work with this kind of random grid and don't use the naive random grid.

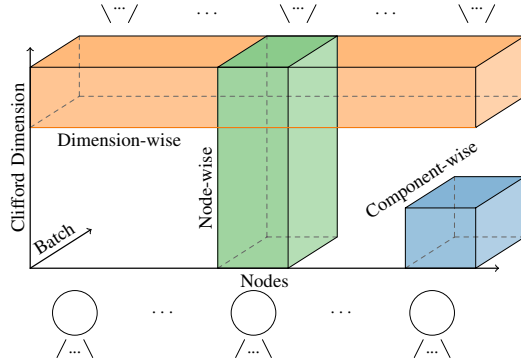


Fig. 3: Visualization of *dimension-wise* (orange), *node-wise* (green) and *component-wise* (blue) batch normalization.

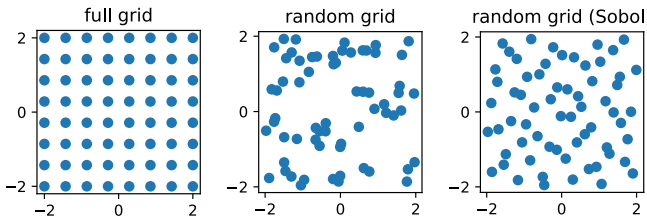


Fig. 2: Comparison of full grid, random grid, and quasi-random Sobol grid using Sobol sequences with 64 grid points each.

#### D. Expressivity of Sobol-CliffordKAN

Using the uniform grid does not scale in high-dimensional space, however, using a uniform random grid results in very high variance. By introducing the *Sobol grid*, we reduce the variance of the model (4). We now analyze the properties of the proposed approach. A  $(t, m, d)$ -net in base  $b$ , with  $0 \leq t \leq m$ , is a set of samples  $y_1, \dots, y_{b^m} \in [0, 1]^d$  such that for each hyper-cube of volume  $b^{t-m}$  it contains exactly  $b^t$  points. Here, the total number of points is called  $n = b^m = |G|$ , while in the rest of the paper  $n$  is the dimension of the vector space. We now consider the integral  $h(x) = \int_{[0,1]^d} g(y)k(x-y)dy$ . If we sample  $\{y_i\}_{i \in [n]}$  in  $[0, 1]^d$ , we can use Monte Carlo (MC) to estimate  $h(x) \approx \frac{1}{n} \sum_{i=1}^n g(y_i)k(x-y_i) = \hat{h}_n(x)$ . We notice that (4)  $\Phi(x) = \sum_{g \in G} w_g \phi(x-g) = \hat{h}_n(x)$ , with  $g(y_i) = w_g$  and  $k(x-y_i) = \phi(x-y_i)$ . If we denote  $\sigma^2(h(x)) = \mathbb{E}[\|h(x) - \mu(x)\|_\infty^2]$ , it follows that:

**Property IV.1.** *If the grid points are generated using a scrambled  $(t, m, d)$ -net in base  $b$  [35], [36], and  $g(y), k(x)$  are smooth functions, s.t.  $f_x(y) = g(y)k(x-y) \in L^{1+\epsilon}[0, 1]^d$ ,  $\epsilon > 0$ , then*

$$\mathbb{E}[\|\hat{h}_n(h(x)) - \mu(h(x))\|_\infty^2] \leq \Gamma \frac{\sigma^2(h(x))}{n} = O(n^{-1}). \quad (5)$$

*Proof:* We apply the result of [35], [37] to the integration of function  $f_x(y) = g(y)k(x-y)$ .  $\mathbb{E}[\|\hat{h}_n^x - \mu_x\|^2] \leq \Gamma \frac{\sigma_x^2}{n}$ , with  $\sigma_x^2 = \sigma^2(f_x) = \mathbb{E}[\|f_x(y) - \mu_x\|^2]$ ,  $\forall x \in [0, 1]^d$ , and  $\hat{h}_n^x = \frac{1}{n} \sum_{i=1}^n f_x(y_i)$ . This is also true for the maximum of the variances, and therefore the result follows. ■

We can now state our lemma

**Lemma IV.2.** *If we use the Sobol grid of size  $n$ , then  $\Phi(x) = \sum_{g \in G} w_g \phi(x-g)$  is an unbiased estimator of  $h(x) = \int_{[0,1]^d} g(y)\phi(x-y)dy$  with variance  $O(n^{-1})$ .*

*Proof:* Using the Sobol scrambled sequence, we define the estimator of  $h(x)$  with the condition in Pr. IV.1 as  $\hat{h}_n(x) = \frac{1}{n} \sum_{i=1}^n g(y_i)k(x-y_i)$ . As before, we rewrite  $\Phi(x) = \sum_{g \in G} w_g \phi(x-g) = \hat{h}_n(x)$ , with  $g(y_i) = w_g$  and  $k(x-y_i) = \phi(x-y_i)$ . Therefore, from Pr. IV.1, we have that  $\Phi(x)$  is an unbiased estimator  $h(x)$  with variance  $O(n^{-1})$ . ■

Therefore, training our KAN network means training the function  $g(y)$ , evaluated at the grid points. Our proposed Sobol-CliffordKAN can learn any function that can be written as a convolution with the kernel  $\phi(x)$  with an error of  $O(n^{-1})$ . We further notice that with this interpretation, the role of the kernel is to smooth the learned function  $g(y)$ , and for the limit of  $\beta \rightarrow \infty$  and  $n \rightarrow \infty$ , we recover the original function, if we consider the new kernel  $k(x) = \beta/\sqrt{\pi}\phi(\beta x) \rightarrow_{\beta \rightarrow \infty} = \delta(x)$ .

#### E. Batch normalization

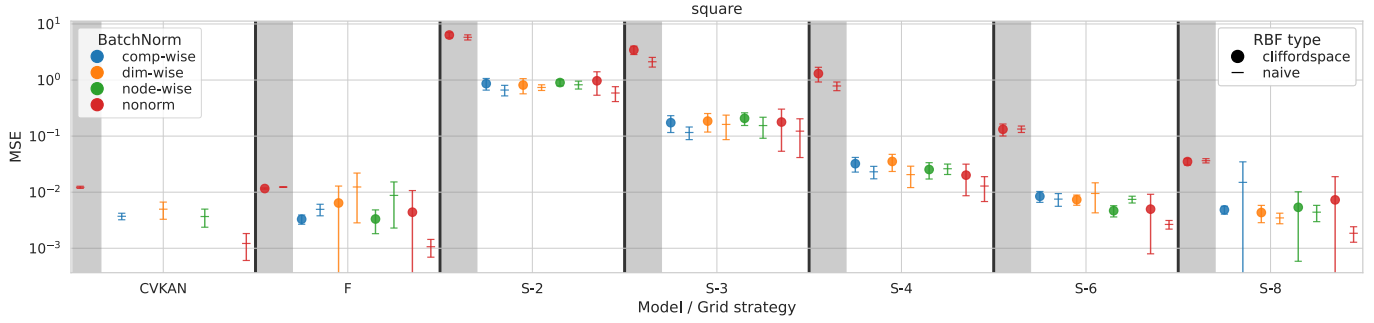
Since the batch normalization approaches of CVKAN only consider complex numbers [7], we introduce three types of normalization for the arbitrarily high dimensional Clifford algebras (see Fig. 3), to make sure inputs to the next layer of our ClKAN likely stay within the grid ranges:

- *Dimension-wise* batch normalization applies batch normalization over each individual dimension of all nodes in one layer combined.
- In *node-wise* batch normalization we normalize the input in each single node of the KAN architecture over all its dimensions at once. This approach is intuitively the best fitting approach for KANs, as each node can compute different correlations in the data and therefore each node's output should be normalized independently of other nodes in the same layer.
- *Component-wise* batch normalization is a combination of *dimension-wise* and *node-wise* batch normalization, as each node and each dimension get normalized independently over all samples in the batch.

Additionally *no-normalization* can be applied, but then there is a high chance that inputs into the next layer exceed the grid ranges and are far away from every grid point, so that the node's output for such out of range data is 0.

## V. EXPERIMENTS

In all of our experiments we applied a 5-fold cross-validation, where we also re-initialized the weights and *Sobol grids* for each run, and used a validation loss plateau scheduler with an initial learning rate of 0.1 - in contrast to [7] who used a learning rate of 0.01 -, a reduction factor 0.9, patience of 20 epochs and a threshold of 0.001. We also applied early stopping after the validation loss has not decreased by at least 0.001 in the last 200 epochs. For the full grid approach we adapted the number of grid points per dimension  $D$  from



(a) *square* (6a) dataset.



(b) *squaresquare* (6d) dataset.

Fig. 4: Overview of Mean Square Error (MSE) for all experiments for complex-valued synthetic function fitting tasks on formulas (6a) and (6d) with color indicating the type of batch normalization, shape the type of RBF and shading the architecture size with shaded regions representing the small model architecture. X-axis labels correspond to CVKAN baseline, Full grid and *Sobol grid* with number of grid points per dimension. For better readability S-5 and S-7 have been omitted. Y-axis shown in log-scale.

CVKAN as 8, so that the total number of grid points is  $(N_g)^D = 8^D$ . For the *Sobol grid* we selected 2 to 8 grid points per dimension to study the minimum required number of random grid points for similar performance as full grid. We also chose grid ranges of  $[-2, 2]$  for each dimension compliant with CVKAN. For all regression tasks we trained on MSE and evaluated on the MSE and Mean Average Error (MAE) metric, while for classification tasks we used Cross-Entropy (CE) for training and additionally evaluated the accuracy.

#### A. Complex-valued basic synthetic formulas

First, we evaluated if our  $\mathbb{C}lKAN$  achieves the same performance as CVKAN on simple complex-valued function-fitting tasks. Therefore we compare our network against CVKAN on datasets generated by the four complex-valued synthetic formulas *square* (6a), *sin* (6b), *mult* (6c) and *squaresquare* (6d), just like Wolff et al. [7]. We use 5000 samples for train- and validation-split combined and another 5000 samples for test-split and adapt the same architecture sizes as [7]. For uni-variate functions (6a) and (6b) we use KAN architectures of sizes  $[1, 1]$  and  $[1, 2, 1]$ , for bi-variate functions *mult* (6c)  $[2, 2, 1]$  and  $[2, 4, 2, 1]$  and for *squaresquare* (6d)  $[2, 1, 1]$  and  $[2, 4, 2, 1]$ .

$$f_1(x) = x^2 \quad (6a) \quad f_3(x_1, x_2) = x_1 \cdot x_2 \quad (6c)$$

$$f_2(x) = \sin(x) \quad (6b) \quad f_4(x_1, x_2) = (x_1^2 + x_2^2)^2 \quad (6d)$$

#### B. Complex-valued larger datasets

We also evaluated on larger datasets more connected to the real-world. We used the same complex-valued *holography* (7) dataset from CVKAN with 100.000 samples for train and validation split combined and another 100.000 samples for the test split. This formula is motivated by holography from physics, as the inputs into the function are a reference beam with electric field strength  $E_R$ , an object beam  $E_0$  and a reconstruction beam  $\widehat{E}_R$  used to reconstruct a hologram  $H$

$$H = \widehat{E}_R \cdot |E_R + E_0|^2 \quad (7)$$

with  $H, \widehat{E}_R, E_R, E_0 \in \mathbb{C}$ . Additionally we briefly analyzed the performance on the *knot* dataset [38], which was also used for evaluation in CVKAN.

#### C. Higher-dimensional Clifford algebras

To analyze how our  $\mathbb{C}lKAN$  performs in higher dimensions than complex, we trained on datasets also generated by the formulas (6a), (6c) and (6d) but with  $x, x_1, x_2 \in \mathbb{C}l(p, q, r)$ . We evaluate the performance on key Geometrical Algebras: 1) Euclidean GA over  $\mathbb{R}^2$ , i.e.  $\mathbb{C}l(2)$ , 2) the quaternion isomorphic  $\mathbb{C}l(0, 2)$ , 3) the zero dimensional Conformal GA  $\mathbb{C}l(1, 1)$ , and 4) the one dimensional Projective Geometric Algebra (PGA)  $\mathbb{C}l(1, 0, 1)$ .

TABLE I: Comparison of the Best Performing Model (MSE) for Each of the Four Complex-valued Function Fitting Tasks. Values for Che et al. [8] and Wolff et al. with lr=0.01 [7] Copied from Their Respective Paper. Values for  $\mathbb{C}/\text{KAN}$  Stem from the Best Models Across All RBF, Batch Normalization and Grid Strategies and All Evaluated Architecture Sizes.

Dataset	CVKAN		improved CVKAN [8]	$\mathbb{C}/\text{KAN}$
	lr=0.01 [7]	lr = 0.1		
square	0.013	0.001	0.009	0.001
sin	0.005	0.001	0.005	0.001
mult	0.045	0.005	0.029	0.002
squaresquare	8.150	1.665	7.355	2.049

Because the underlying Clifford algebras are four-dimensional in contrast to the previously used two-dimensional complex values, we need more data points to cover the space sufficiently. For complex-valued function fitting we sampled 5000 data points in a range  $[-2, 2]$  for each dimension. Therefore, we had a sampling density of  $\frac{5000}{4^2}$ . In order to achieve the same sampling density in a four-dimensional hypercube, we need  $\frac{N}{4^4} = \frac{5000}{4^2}$  and therefore  $N = 16 \cdot 5000 = 80000$  samples instead for combined train- and validation- as well as test-split.

We ran experiments with the most promising batch normalization and RBF computation strategy given by the previous experiments (cf. Section V-A). Furthermore we conducted exhaustive experiments for grid type and number of random grid points, to see how well our proposed *Sobol grid* approach behaves in higher dimensions.

## VI. RESULTS

In this section we will show and describe the most interesting results. We omit the plot for complex-valued function fitting on *sin* (6b) and *mult* (6c) dataset and leave out *Sobol grids* with  $N_g \in \{5, 7\}$  for better readability. We will make all the results available in a machine readable way together with additional plots and tables inside our repository for the code base.

### A. Comparison to baseline

First we want to compare our  $\mathbb{C}/\text{KAN}$  to the baseline CVKAN as well as to its improved version [8]. Table I compares the best performing model from CVKAN by Wolff et al. [7], improved CVKAN by Che et al. [8] and our  $\mathbb{C}/\text{KAN}$  for each complex-valued function fitting dataset. It should be noted that in contrast to CVKAN that used 5000 data points for 5-fold cross-validation training and reported validation losses, we introduce an additional test split of the same size and report test losses but still only do training and cross-validation on 5000 data points. This dataset setup was used for CVKAN with lr=0.1 and our  $\mathbb{C}/\text{KAN}$ . It can be seen that the increased learning rate of 0.1 makes the results of CVKAN far better and that our  $\mathbb{C}/\text{KAN}$  achieves similar results with the same learning rate. The improved version of CVKAN is better than standard CVKAN with 0.01 learning rate, but can not keep up with the finer tuned learning rate.

### B. Complex-valued basic synthetic formulas

Fig. 4a and Fig. 4b show that our full grid  $\mathbb{C}/\text{KAN}$  performs similarly well as CVKAN with the same number of parameters. The performance of the *Sobol grid* strategy gets better with an increasing amount of grid points per dimension and for  $N_g = 8$  grid points per dimension the *Sobol grid* approach is on par with the full uniform grid. The larger architectures perform consistently better than smaller architectures. Fig. 4a has smaller shaded regions and showcases only batch normalization *no-normalization* for small architectures because the small architecture size for the *square* dataset is  $[1, 1]$  and we never apply batch normalization on the final output of the model. Therefore, other batch normalization approaches than *no-normalization* are not applicable for this architecture size.

For the choice of RBF calculation the naive (1a) and Clifford approach (1b) perform similarly well. When comparing the different batch normalization approaches no clear winner can be spotted. In some cases (e.g. *square*, full grid and naive RBF with the big architecture in Fig.4a) *no-normalization* performs best, in other cases (e.g. *squaresquare*, full grid and Clifford RBF with the big architecture in Fig.4b) *node-wise* or *dim-wise* batch normalization are the best choice.

TABLE II: Comparison of CVKAN and  $\mathbb{C}/\text{KAN}$  on the Holography Dataset (7) for the Two Largest Architectures and Node-wise Batch Normalization. Choice of RBF is Clifford RBF (1b) for  $\mathbb{C}/\text{KAN}$ . GT=Grid Type  $\in \{\text{Full Grid and Sobol Grid}\}$ ,  $N_g$  = Number of Grid Points per Dimension,  $N_p$ =# Parameters

Model	$N_p$	GT	$N_g$	Test MSE	Test MAE
$3 \times 10 \times 3 \times 1$					
$\mathbb{C}/\text{KAN}$	8342	F	8	<b>0.021</b> $\pm 0.003$	<b>0.090</b> $\pm 0.011$
	8342	F	8	<b>0.030</b> $\pm 0.005$	<b>0.092</b> $\pm 0.008$
	782	S	2	2.799 $\pm 0.780$	1.211 $\pm 0.167$
	1412	S	3	0.713 $\pm 0.135$	0.602 $\pm 0.069$
	2294	S	4	0.275 $\pm 0.133$	0.348 $\pm 0.099$
	3428	S	5	0.101 $\pm 0.030$	0.192 $\pm 0.034$
	4814	S	6	0.070 $\pm 0.019$	0.154 $\pm 0.031$
	6452	S	7	0.043 $\pm 0.006$	0.117 $\pm 0.009$
	8342	S	8	0.036 $\pm 0.008$	0.111 $\pm 0.012$
$3 \times 10 \times 5 \times 3 \times 1$					
$\mathbb{C}/\text{KAN}$	12972	F	8	<b>0.016</b> $\pm 0.001$	<b>0.066</b> $\pm 0.003$
	12972	F	8	<b>0.025</b> $\pm 0.004$	<b>0.069</b> $\pm 0.006$
	1212	S	2	1.891 $\pm 0.275$	0.952 $\pm 0.078$
	2192	S	3	0.272 $\pm 0.036$	0.358 $\pm 0.022$
	3564	S	4	0.093 $\pm 0.021$	0.179 $\pm 0.017$
	5328	S	5	0.059 $\pm 0.012$	0.123 $\pm 0.010$
	7484	S	6	0.041 $\pm 0.006$	0.100 $\pm 0.012$
	10032	S	7	0.029 $\pm 0.004$	0.081 $\pm 0.005$
	12972	S	8	0.028 $\pm 0.004$	0.079 $\pm 0.003$

### C. Complex-valued larger datasets

The results on the holography dataset (7) in Table II show that  $\mathbb{C}/\text{KAN}$  with full grid and *Sobol grid* with  $N_g = 8$  and the baseline CVKAN perform similarly well. For the *Sobol grids* with  $N_g = 7$ , and therefore  $\approx 75\%$  of parameters, the test MSE is almost the same compared to a full grid model. With

TABLE IV: Comparison of  $\mathbb{C}l(1, 0, 1)$  for *square* and *squaresquare* Datasets, Largest Architectures and *node-wise* Batch Normalization. Choice of RBF is Clifford RBF (1b). GT=Grid Type  $\in \{\text{Full Grid and Sobol Grid}\}$ ,  $N_g$  = Number of Grid Points per Dimension,  $N_p$ =# Parameters.

$N_p$	GT	$N_g$	Test MSE	Test MAE
<i>square</i>				
			$1 \times 2 \times 1$	
65572	F	8	$0.968 \pm 0.834$	$0.585 \pm 0.381$
292	S	2	$0.054 \pm 0.018$	$0.187 \pm 0.032$
1332	S	3	<b><math>0.004 \pm 0.001</math></b>	<b><math>0.054 \pm 0.005</math></b>
4132	S	4	$0.006 \pm 0.004$	$0.058 \pm 0.020$
10036	S	5	$0.102 \pm 0.199$	$0.148 \pm 0.217$
20772	S	6	$0.177 \pm 0.171$	$0.270 \pm 0.196$
38452	S	7	$0.027 \pm 0.042$	$0.096 \pm 0.079$
65572	S	8	$0.045 \pm 0.076$	$0.114 \pm 0.105$
<i>squaresquare</i>				
			$2 \times 4 \times 2 \times 1$	
295068	F	8	$33.586 \pm 32.646$	$3.492 \pm 2.202$
1308	S	2	$20.578 \pm 6.499$	$3.194 \pm 0.481$
5988	S	3	$1.685 \pm 0.367$	$0.900 \pm 0.108$
18588	S	4	$0.445 \pm 0.074$	$0.453 \pm 0.035$
45156	S	5	$0.270 \pm 0.082$	$0.345 \pm 0.054$
93468	S	6	<b><math>0.178 \pm 0.052</math></b>	<b><math>0.285 \pm 0.036</math></b>
173028	S	7	$0.203 \pm 0.077$	$0.304 \pm 0.063$
295068	S	8	$1.425 \pm 2.414$	$0.609 \pm 0.557$

very low number of grid points  $N_g \in \{2, 3, 4\}$  the model can not approximate the underlying function of the dataset well.

When comparing the different batch normalization approaches in Table III, it can be clearly seen that *no normalization* performs by far the worst and the model is not able to learn anything. The other three approaches for batch normalization perform on par with very low differences between them.

We also analyzed the performance of our model on the knot dataset (Section V), but the accuracies of all models regardless of grid strategy and grid size were so close to each other and mostly above 90% that we chose not to include the results as they would not give additional insight to recognize differences between the candidates.

#### D. Higher-dimensional Clifford algebras

Fig. 5 shows all experiments on higher-dimensional Clifford algebras. Similar to Section VI-B, *Sobol grid* with the same number of parameters performs approximately as good as the full grid approach. However, in this four-dimensional Clifford algebra, the *Sobol grid* experiments with  $N_g \in \{3, 4\}$  show very promising results with a drastically reduced number of parameters ( $\approx 2 - 6\%$  of parameters). Overall, the *mult* (6c) and *square* (6a) datasets can be learned with a lower MSE than *squaresquare* (6d) dataset. The  $\mathbb{C}l(1, 0, 1)$  profits the most from the *Sobol grid* approach and shows even better performance with  $N_g = 4$  than for the full grid.

In Table IV it is shown, that for  $\mathbb{C}l(1, 0, 1)$  and the *square* and *squaresquare* dataset the results of *Sobol grid* are consistently better than full grid. Some grid sizes, e.g.  $N_g \in \{5, 6\}$  for *square* and  $N_g = 8$  for *squaresquare*, perform worse than other grid sizes with high standard deviations.

#### E. Discussion

In our experiments (Section VI) we found out that the way of calculating the RBFs does not seem to have a big influence on the model's performance, while the type of batch normalization to use depends on the dataset and there can be cases where *no-normalization* at all seems beneficial, while in other cases models without batch normalization don't train at all. If normalization is helpful, the concrete type of batch

TABLE III: Comparison of Batch Normalization Schemes for CVKAN and  $\mathbb{C}l$ KAN on the Holography Dataset (7) for the Biggest Architecture [3, 10, 5, 3, 1] and Full Grid with  $N_g = 8$ . Choice of RBF is Clifford RBF (1b) for  $\mathbb{C}l$ KAN.

Model	Norm	Test MSE	Test MAE
CVKAN	nodew.	$0.016 \pm 0.001$	$0.066 \pm 0.003$
	dimw.	$0.015 \pm 0.003$	$0.062 \pm 0.008$
	compw.	$0.017 \pm 0.002$	$0.063 \pm 0.004$
	no	$51.059 \pm 62.526$	$3.278 \pm 3.951$
$\mathbb{C}l$ KAN	nodew.	$0.025 \pm 0.004$	$0.069 \pm 0.006$
	dimw.	$0.021 \pm 0.003$	$0.060 \pm 0.005$
	compw.	$0.028 \pm 0.009$	$0.071 \pm 0.006$
	no	$0.867 \pm 1.061$	$0.354 \pm 0.382$

normalization - be it *node-wise*, *dimension-wise* or *component-wise* - does not matter much.

The *squaresquare* dataset is by far the most challenging one to train on. We suspect this depends on the large variability of its output values, compared to *square*. We noticed very early in our experiments that CVKAN as well as  $\mathbb{C}l$ KAN were highly dependent on a good initialization. Therefore, we have increased the learning rate by a factor of 10 to a value of 0.1 in comparison to [7]. This enables the models to drift further away from the weights given by random initialization and therefore reach more favorable regions. The results across different training runs and during crossfold-validation also became more stable. This small change alone allowed us to already beat the improved CVKAN [8] by a lot.

For higher dimensions (Section VI-C) we have shown that our proposed *Sobol grid* can be a good tool for parameter reduction in higher dimensions to mitigate the otherwise exponential growth of parameters for the full grid. Some Clifford algebras, e.g.  $\mathbb{C}l(1, 0, 1)$ , even benefit from the *Sobol grid* approach in terms of accuracy with drastically reduced parameters. Although it must be noted that *Sobol grid* sometimes also produces worse results than full grid and some grid sizes in our experiments for specific datasets produce high standard deviations. This is a general discovery in the experiments, since some experimental setups, that should work in theory, only work for some cross-validation runs in practice therefore producing high MSE on average and a high standard deviation. With the increased learning rate the experiments overall became more stable and reproducible across runs, but some instabilities can still be observed across all tasks.

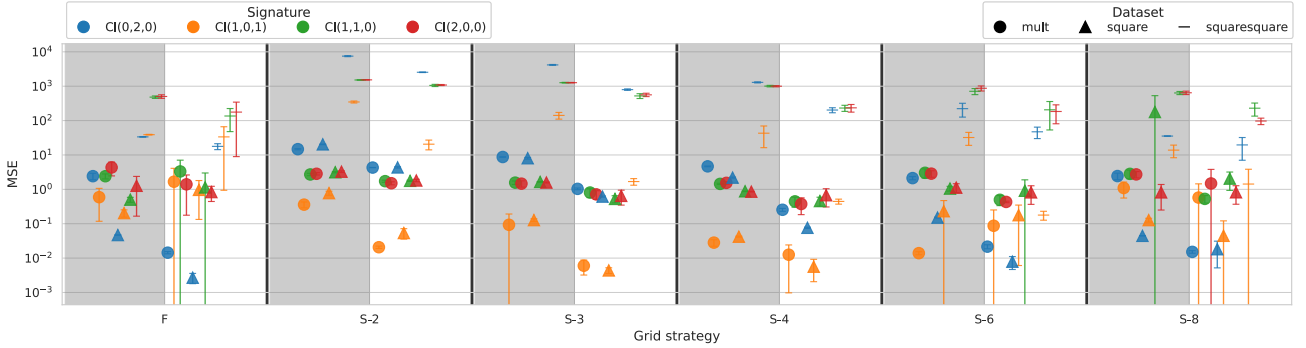


Fig. 5: Function-fitting experiments on higher dimensional Clifford algebras. Color represents Clifford algebra used, shape the dataset *mult* (6c), *square* (6a) and *squaresquare* (6d) and shading the model architecture per dataset with shaded regions representing the small model architecture. X-axis labels correspond to **Full grid** and ***Sobol grid*** with number of grid points per dimension. For better readability S-5 and S-7 have been omitted. Y-axis shown in log scale.

## VII. CONCLUSION

We have shown that our  $\mathbb{C}/\text{KAN}$  achieves similar performance on complex-valued datasets compared to CVKAN as a baseline. Additionally, we have demonstrated that  $\mathbb{C}/\text{KAN}$  can also be successfully applied in higher dimensions for function fitting tasks.

Furthermore, we have shown that our introduced *Sobol grid* can be used to mitigate the curse of dimensionality for higher dimensional Clifford algebras, where a conventional full uniform grid approach would require an exponential number of parameters. Surprisingly, there are cases where the limited number of parameters in a relatively small *Sobol grid* actually benefit the model's performance and lead to better results than the full grid.

Further research could be dedicated in the direction of learnable RBF shape and alternative residual activation functions than SiLU with improved learning rate, similarly to [8] for CVKAN. Additionally, future work could focus on improving the stability of KANs and CVKAN and  $\mathbb{C}/\text{KAN}$  in particular, making them even less dependent on good initializations and more robust across different runs.

## ACKNOWLEDGMENT

LLMs (ChatGPT 5.2 and Google Gemini) were used for sentence-level reformulation, or as search tool, but not for text generation.

## REFERENCES

- [1] A. N. Kolmogorov, *On the representation of continuous functions of several variables by superpositions of continuous functions of a smaller number of variables*. American Mathematical Society, 1961.
- [2] A. Ismayilova and V. E. Ismailov, "On the kolmogorov neural networks," *Neural Networks*, vol. 176, p. 106333, 2024.
- [3] D. A. Sprecher and S. Draghici, "Space-filling curves and kolmogorov superposition-based neural networks," *Neural Networks*, vol. 15, no. 1, pp. 57–67, 2002.
- [4] Z. Liu, Y. Wang, S. Vaidya, F. Ruehle, J. Halverson, M. Soljacic, T. Hou, and M. Tegmark, "KAN: Kolmogorov–arnold networks," in *ICLR*, 2025, pp. 70 367–70 413.
- [5] S. Somvanshi, S. A. Javed, M. M. Islam, D. Pandit, and S. Das, "A survey on kolmogorov–arnold network," *ACM Computing Surveys*, vol. 58, no. 2, pp. 1–35, 2025.
- [6] R. Yu, W. Yu, and X. Wang, "KAN or MLP: A fairer comparison," *arXiv:2407.16674*, 2024.
- [7] M. Wolff, F. Eilers, and X. Jiang, "CVKAN: Complex-valued kolmogorov–arnold networks," in *IJCNN*, 2025, pp. 1–9.
- [8] R. Che, L. af Klinteberg, and M. Aryaapoor, "Improved complex-valued Kolmogorov–Arnold networks with theoretical support," in *24th EPIA Conference on Artificial Intelligence*. Springer Nature Switzerland, 2026, pp. 439–451.
- [9] M.-J. Lai and Z. Shen, "The Kolmogorov superposition theorem can break the curse of dimensionality when approximating high dimensional functions," *arXiv:2112.09963*, 2021.
- [10] T. Poggio, "How deep sparse networks avoid the curse of dimensionality: Efficiently computable functions are compositionally sparse," *CBMM Memo*, vol. 10, p. 2022, 2022.
- [11] M. M. Ferdaus, M. Abdelguerif, E. Ioup, D. Dobson, K. N. Niles, K. Pathak, and S. Sloan, "KANICE: kolmogorov–arnold networks with interactive convolutional elements," in *4th International Conference on AI-ML Systems (AIMLSystems)*, 2024, pp. 13:1–13:10.
- [12] A. D. Bodner, A. S. Tepich, J. N. Spolski, and S. Pourteau, "Convolutional kolmogorov–arnold networks," *arXiv:2406.13155*, 2024.
- [13] X. Yang and X. Wang, "Kolmogorov–arnold transformer," in *ICLR*, 2025.
- [14] Z. Kuang, H. Bi, Z. Lv, and C. Xu, "Exploring complex-valued convolutional Kolmogorov–Arnold networks for PolSaR image classification," in *IEEE International Geoscience and Remote Sensing Symposium*, 2025, pp. 1945–1949.
- [15] L. Hu, Y. Wang, and Z. Lin, "Incorporating arbitrary matrix group equivariance into KANs," in *ICML*, 2025.
- [16] F. Alesiani, T. Maruyama, H. Christiansen, and V. Zaverkin, "Geometric Kolmogorov–Arnold Superposition Theorem," *arXiv:2502.16664*, 2025.
- [17] F. Alesiani, H. Christiansen, and F. Errica, "Variational kolmogorov–arnold network," *arXiv:2507.02466*, 2025.
- [18] Z. Liu, M. Tegmark, P. Ma, W. Matusik, and Y. Wang, "Kolmogorov–arnold networks meet science," *Phys. Rev. X*, vol. 15, p. 041051, 2025.
- [19] R. C. Yu, S. Wu, and J. Gui, "Residual kolmogorov–arnold network for enhanced deep learning," *arXiv:2410.05500*, 2024.
- [20] D. Lundholm and L. Svensson, "Clifford algebra, geometric algebra, and applications," *arXiv:0907.5356*, 2009.
- [21] J. Brandstetter, R. van den Berg, M. Welling, and J. K. Gupta, "Clifford neural layers for pde modeling," in *ICLR*, 2023.
- [22] J. Brehmer, P. De Haan, S. Behrends, and T. Cohen, "Geometric algebra transformers," in *NeurIPS*, 2023.
- [23] D. Ruhe, J. Brandstetter, and P. Forré, "Clifford group equivariant neural networks," *NeurIPS*, pp. 62 922–62 990, 2023.
- [24] D. Ruhe, J. K. Gupta, S. De Keninck, M. Welling, and J. Brandstetter, "Geometric Clifford algebra networks," in *ICML*, 2023, pp. 29 306–29 337.
- [25] E. Bayro-Corrochano, L. Reyes-Lozano, and J. Zamora-Esquivel, "Conformal geometric algebra for robotic vision," *Journal of Mathematical Imaging and Vision*, vol. 24, pp. 55–81, 2006.

- [26] D. Hildenbrand, J. Zamora, and E. Bayro-Corrochano, “Inverse kinematics computation in computer graphics and robotics using conformal geometric algebra,” *Advances in applied Clifford algebras*, vol. 18, pp. 699–713, 2008.
- [27] L. Dorst and S. Mann, “Geometric algebra: a computational framework for geometrical applications,” *IEEE Computer Graphics and Applications*, vol. 22, no. 3, pp. 24–31, 2002.
- [28] A. Crumeyrolle, *Orthogonal and symplectic Clifford algebras: Spinor structures*. Springer Science & Business Media, 2013, vol. 57.
- [29] J. M. Chappell, S. P. Drake, C. L. Seidel, L. J. Gunn, A. Iqbal, A. Allison, and D. Abbott, “Geometric algebra for electrical and electronic engineers,” *Proceedings of the IEEE*, vol. 102, no. 9, pp. 1340–1363, 2014.
- [30] D. Hestenes and A. Lasenby, *Space-time algebra*. Springer, 2015.
- [31] J. Moody and J. Usevitch, “Automatic grid updates for Kolmogorov-Arnold networks using layer histograms,” *arXiv:2511.08570*, 2025.
- [32] L. N. Zheng, W. E. Zhang, L. Yue, M. Xu, O. Maennel, and W. Chen, “Free-knots Kolmogorov-Arnold network: On the analysis of spline knots and advancing stability,” *arXiv:2501.09283*, 2025.
- [33] J. Bergstra and Y. Bengio, “Random search for hyper-parameter optimization,” *Journal of Machine Learning Research*, vol. 13, no. 10, pp. 281–305, 2012.
- [34] I. M. Sobol’, “The distribution of points in a cube and the accurate evaluation of integrals,” *Zhurnal Vychislitel’noi Matematiki i Matematicheskoi Fiziki*, vol. 7, no. 4, pp. 784–802, 1967.
- [35] A. B. Owen and D. Rudolf, “A strong law of large numbers for scrambled net integration,” *SIAM Review*, vol. 63, no. 2, pp. 360–372, 2021.
- [36] A. B. Owen, “Scrambling Sobol’ and Niederreiter-Xing points,” *Journal of Complexity*, vol. 14, no. 4, pp. 466–489, 1998.
- [37] ———, “Randomly permuted (t, m, s)-nets and (t, s)-sequences,” in *Monte Carlo and Quasi-Monte Carlo Methods in Scientific Computing*. Springer, 1995, pp. 299–317.
- [38] A. Davies, P. Veličković, L. Buesing, S. Blackwell, D. Zheng, N. Tomašev, R. Tanburn, P. Battaglia, C. Blundell, A. Juhász *et al.*, “Advancing mathematics by guiding human intuition with AI,” *Nature*, vol. 600, no. 7887, pp. 70–74, 2021.